Kinetic Properties of Enzyme Populations in Vivo: Alkaline Phosphatase of the *Escherichia coli* Periplasm†

Michael B. Martinez,‡ Fred J. Schendel,§ Michael C. Flickinger,§ and Gary L. Nelsestuen*,‡

Department of Biochemistry, University of Minnesota, 1479 Gortner Avenue, St. Paul, Minnesota 55108

Received May 28, 1992; Revised Manuscript Received September 2, 1992

ABSTRACT: Studies were conducted to determine the role that diffusion may play in the in vivo kinetics of the *Escherichia coli* periplasmic enzyme, alkaline phosphatase (AP, encoded by the gene *pho A*). Passive diffusion of solutes, from solution into the periplasm, is thought to occur mainly through porins in the outer membrane. The outer membrane therefore serves as a diffusion barrier separating a population of periplasmic enzymes from bulk substrate. *E. coli* strains containing a plasmid with the *pho A* gene linked to the *lac* promoter were used in this study in order to vary the amount of enzyme per cell. Alkaline phosphatase assays were conducted with intact cells, and the substrate concentration at half-maximum velocity (normally the K_m for the enzyme) was determined as a function of enzyme concentration per cell. The results showed that diffusion of substrate to the enzyme caused as much as a 1000-fold change in this parameter, compared to that of purified enzyme. This suggested that diffusion was the rate-limiting step of the enzymatic reaction in these cells. In agreement with this type of reaction, Eadie–Hofstee and Lineweaver–Burk plots were not linear. At their extremes, these plots represented two types of kinetics. At high substrate concentration, equilibrium of substrate between bulk solution and the periplasm was achieved, and the kinetic properties conformed to Michaelis–Menten. At low substrate concentrations, there were a large number of free (unbound) enzymes, and each substrate molecule that entered the periplasm, through the diffusion barrier, resulted in product formation. In the latter case, the periplasm behaved as a perfectly reactive vessel, and enzyme velocity increased in direct proportion to substrate concentration. This is a useful kinetic approach to estimate diffusion rates through the outer membrane. Diffusion rates can be valuable for investigating variation in expression and permeability of porins in the outer membrane. This study shows how, in vivo, the conditions required for Michaelis–Menten analysis of enzyme kinetics are not met and more complex behavior is observed.

Enzyme kinetics in a purified system is a common method for studying enzyme mechanism, and observed properties are often used for comparison to in vivo reactions. However, there are major differences between in vitro enzyme reaction conditions and the in vivo milieu of the cell, the enzymes normal environment. For example, in vitro individual enzyme molecules are dissolved in buffer and are usually at low concentrations. In contrast, the in vivo environment may consist of highly dense populations of enzymes (sequestered or compartmentalized) with low substrate concentrations. In Gram-negative bacteria, intracellular as well as periplasmic enzymes represent significant states of inhibited diffusion of substrate to the vicinity of a population of enzymes. These in vivo factors may cause deviation from the behavior of an enzyme in a purified system and may even be involved in regulation of enzyme activity. Thus, how in vivo conditions alter enzyme kinetic behavior is an interesting question.

In dilute solutions, the interaction of substrate with an enzyme is described by diffusion of substrate to a single enzyme site, binding to that site, and catalysis. However, if a dense population of enzymes exists in a constrained environment, illustrated by attachment to a large particle, they can function as a perfectly reactive region and convert all substrates that collide to product. In this case, the interaction of substrate with enzyme is determined by diffusion of substrate to the population of enzymes, and reaction velocity becomes a property of the entire population rather than of individual sites. As outlined by Abbott and Nelsestuen (1988), enzymes in this situation should display a K_m that varies with the nature of the enzyme population (e.g., number of enzymes/population) and which is independent of the nature of the enzyme active site. This behavior can apply to enzymes grouped on a region of a surface or to a group of enzymes sequestered behind a diffusion barrier. The latter can be described essentially as a vessel with limited access. The only requirement for this behavior is that a population of enzymes act as a perfectly reactive surface or vessel and capture a significant proportion of substrates that collide or enter.

A convenient model for examing the impact of an enzyme population and diffusion barriers on enzyme activity consists of intact bacteria. The outer membrane of the Gram-negative bacteria *Escherichia coli* contains porins that serve as channels for diffusion of small solutes into the periplasm (Nikaido & Vaara, 1985), the space between the inner and outer membranes (Stock et al., 1977). The periplasm contains several enzymes which are expressed under different growth conditions (Beacham, 1979). The three major porins of the outer membrane, Omp C, Omp F, and Pho E, have been investigated extensively by in vitro methods (Nakae et al., 1979; Nikaido & Rosenberg, 1983; Datta et al., 1977).

There is considerable evidence suggesting that the outer membrane and various porins serve regulatory functions for the cell. Pho E is expressed when cells are grown under conditions of phosphate starvation, with coexpression of the periplasmic enzyme alkaline phosphatase (Argast & Boos,

† Supported in part by Grants HL 15728 (to G.L.N.) from the National Institutes of Health and NSF/ECF8618134 (to M.C.F.) from the National Science Foundation.

‡ Department of Biochemistry, University of Minnesota.

§ Department of Biochemistry and Institute for Advanced Studies in Biological Process Technology, University of Minnesota. Current address for F.J.S. is Qualitech Inc., Chaska, MN 55318.

0006-2960/92/0431-11500$03.00/0

1980; Tommassen & Lugtenberg, 1980). Expression of Omp F occurs at low temperature or at low osmolarity. Omp C, on the other hand, is expressed at high temperature or high osmolarity (Alphen & Lugtenberg, 1977). Studies have shown that the combined number of Omp C and Omp F porins per bacterium remains relatively constant regardless of which porin is expressed (Lugtenberg et al., 1976). There is a 3.4-fold increase in Omp C synthesis and a 2-fold decrease in Omp F synthesis upon a shift from low to high osmolarity (Jovanovich et al., 1988). The physiological significance of this shift in porin synthesis is unknown. It has been suggested that porins might have solute charge preferences. Swelling liposome assays and patch clamp methods indicated that Omp C and Omp F have a preference for positively charged compounds while Pho E has a preference for negatively charged compounds (Nikaido & Rosenberg, 1983; Korteland et al., 1984).

Rate-limiting diffusion of compounds across the outer membrane of *E. coli* appears to have been observed (Alphen et al., 1978). For example, it was found that antibiotic effectiveness might be related to outer membrane permeability (Zimmerman & Rosselet, 1977; Nikaido & Nakae, 1979). Sensitivity of the outer membrane has been suggested to explain some effects of detergents, polycations, buffer, and other disorganizing compounds on bacteria (Vaara & Vaara, 1983).

This study investigated diffusion of substrates across the outer membrane to the periplasmic enzyme alkaline phosphatase. Variation of the amount of enzyme allowed us to investigate the influence of enzyme population size on reaction kinetics. The results showed a large variation in the substrate concentration required for half-maximum activity depending on enzyme concentration per cell. This illustrated that this enzyme system, under some conditions, was limited by substrate diffusion and could not be described by a simple K_m. A modified equation for receptor–ligand association rates (Berg & Purcell, 1977) was used to describe enzyme behavior for this in vivo system. It is possible that similar kinetic properties will apply to other enzyme systems, in vivo. A preliminary report of some of the results has been presented (Martinez et al., 1992).

MATERIALS AND METHODS

Media and Reagents. *p*-Nitrophenyl phosphate, isopropyl β-D-thiogalactoside (IPTG),[1] 5-bromo-4-chloro-3-indoyl phosphate, highly purified alkaline phosphatase from *E. coli*, and other chemicals were purchased from the Sigma Chemical Co.

Tryptone broth contained 10 g of Bactopeptone and 5 g of NaCl per liter (Adler, 1973). TB (terrific broth, 1 L) contained 4 g of glycerol, 100 mL of phosphate mixture, 24 g of tryptone, and 12 g of yeast extract (Tartof & Hobbs, 1987). Phosphate mixture contained 0.17 M KH_2PO_4 and 0.72 M K_2HPO_4. LB (Luria Bertani, 1 L) consisted of 10 g of tryptone, 5 g of yeast extract, 5 g of NaCl, and 1.0 mL of 1 N NaOH (Miller, 1972). SOB (1 L) pH 7.5 contained 20 g of tryptone, 5 g of yeast extract, and 0.5 g of NaCl. SOC is SOB containing 1% glucose and 20 mM $MgCl_2$ (Hanahan, 1985). MOPS medium (1 L), pH 7.2 contained 9.2 g of MOPS [3-(*N*-morpholino)propanesulfonic acid], 5.0 g of NaCl, 5.0 g of KCl, and 1.0 g of $(NH_4)_2SO_4$ (Neidhardt et al., 1974). MOPS medium additions were 2.0 mM $MgSO_4$, 1.0 mM K_2HPO_4, 0.1 mM $CaCl_2$, 0.2% glycerol, and trace metals. For agar plates, 15 g/L agar was added to the media. For soft agar 7.5 g/L agar was added. Ampicillin (100 μg/mL) was included in all cultures. IPTG (1 mM) was added to the growth media to induce the *lac* promoter.

Ampicillin selection plates were made using SOC medium and ampicillin (100 μg/mL). Tetracycline selection plates were made using SOB medium containing 1% glucose, 20 mM sodium citrate, and tetracycline (15 μg/mL).

Cell Growth. Cells were inoculated into tryptone broth from a colony on an agar plate or from a freezer culture and allowed to grow overnight at 30 °C in an Orbital shaker (Lab Line) at 300 rpm. Experimental cultures (5 mL of fresh tryptone broth) were inoculated from overnight cultures and grown at 37 °C at 300 rpm. Induction of alkaline phosphatase was accomplished with IPTG (1 mM). Cultures did not exceed an A_{590} of 1.5. An absorbance of 1.0 at 590 nm corresponds to 6×10^8 cells/mL (Adler, 1973), and this value was used to calculate the cell density in the assays. Cells were usually stored overnight on ice and used for experiments the next day. Storage for this period of time did not influence the experimental results.

Strain K12 growth was somewhat modified. Cells were inoculated from a freezer culture into tryptone broth and grown overnight at 37 °C and 300 rpm. Overnight cultures were used to inoculate fresh MOPS media (with additions), and cells were grown to log phase. Cells were washed twice in ice cold MOPS media and resuspended in MOPS media with all additions except phosphate. The cultures were allowed to grow an additional 1.5 h to induce alkaline phosphatase and then were stored on ice for experiments the next day.

On the day cells were used for experiments, they were harvested by centrifugation for 10 min at 3000*g* and then gently resuspended in assay buffer. Resuspended cells were kept on ice until assayed for enzyme activity. Maximum velocity and total enzyme concentration per assay were determined by cell lysis (disrupting the outer membrane) and measurement of enzyme activity using 3.8 mM *p*-nitrophenyl phosphate. This substrate concentration was adequate to provide V_{max} for the total enzyme of the lysed cells. Lysis was accomplished by adding one drop of a 1% sodium deoxycholate solution and one drop of toluene to 0.5 mL of resuspended cells followed by occasional shaking of the suspension for 10 min at 37 °C.

Enzyme Assays. Assays were carried out with a Beckman DU 70 spectrophotometer with readings every 20 s for a total of 2 min. The average of six reaction velocities calculated from absorbance readings, minus background, is the value plotted. The range for these six readings was very low for activity in induced cells and normally less than ±2% of the average. Replicate samples (≥3) were assayed for all V_{max} determinations. The standard deviations were low and less than ±3% of the values reported. Replicate samples were also assayed in the worse case situation where enzyme activity per cell was low so that cell density in the assay was high (wild-type *E. coli*, see below). The standard deviations obtained are shown in Figure 8A. In other cases, which had much lower error, multiple points serve to define the curve shape, and single determinations, obtained from the six continuous readings, are presented without more detailed error estimates.

All components of the assay were warmed to a temperature of 37 °C before mixing. Cells were usually added to the assay mixture last. The total assay volume was 1.0 mL. The cuvettes were placed in the DU 70, equipped with a heated cuvette holder, and allowed to incubate for 50 s before readings were

[1] Abbreviations: IPTG, isopropyl β-D-thiogalactoside; MOPS, 3-(*N*-morpholino)propanesulfonic acid; $[S]_{0.5V_{max}}$, substrate concentration at half V_{max}.

Table I

strains: CGSC[a]	designation	chromosomal markers	plasmid
	MZ9387[b]	*Δlax74Δ, phoA20, phoB⁺, phoR⁻, trp, strA, F', [lacIq lacZ::Tn5 Kmʳ]*	pIV26[c]
	M464E	*[araD139], Δ(argF–lac)205, flbB5301, ptsF25, relA1, rpsL150, ompR321, deoC1, λ⁻, [lacIq lacZ::Tn5 Kmʳ], pho A⁻*	pIV26
	M1157FC	*thr-1, ara-14, leuB6, Δ(gpt–proA)62, lacY1, tsx-33, supE44, galK2, λ⁻, rac⁻, hisG4 (Oc), rbfD1, mgl-51, rpsL31, kdgk51, xyl-5, mtl-1, argE3(Oc) thi-1, [lacIq lacZ::Tn5 Kmʳ] pho A⁻*	pIV26
	M703CE	*proC24, ompF254, his-53, purE41, ilv-277, met-65, lacY29, xyl-14, rpsL97, cycA1, cycB2?, tsx-63, λ⁻, [lacIq lacZ::Tn5 Kmʳ] pho A⁻*	pIV26
6046	JF703[d]	*proC24, ompF254, his-53, purE41, ilv-277, met-65, lacY29, xyl-14, rpsL97, cycA1, cycB2?, tsx-63, λ⁻*	
6780	SG464[d]	*[araD139], Δ(argF–lac)205, flbB5301, ptsF25, relA1, rpsL150, ompR321, deoC1, λ⁻*	
1157	AB1157[e]	*thr-1, ara-14, leuB6, Δ(gpt–proA)62, lacY1, tsx-33, supE44, galK2, λ⁻, rac⁻, hisG4 (Oc), rbfD1, mgl-51, rpsL31, kdgk51, xyl-5, mtl-1, argE3(Oc) thi-1*	
	JF1150[f]	*F', [lacIq lacZ::Tn5 Kmʳ], thr, leu, thi, deo, tonA, lacy, supE44, recA, nalA, nrdA, nrdB*	

[a] Strain number from *E. coli* Genetic Stock Center, Yale University, New Haven, CT. [b] Strain MZ9387 and the plasmid pIV26 were gifts from Fred Schendel, Department of Biochemistry, University of Minnesota. [c] The pIV26 plasmid has been described previously (Schendel et al, 1989). Briefly, it has the *pho A* gene linked to the *lac* promoter, and carries an ampicillin resistance gene. [d] Starting strains, a gift from Greg Pazour, Department of Biochemistry, University of Minnesota, and originally obtained from the *E. coli* Genetic Stock Center, Yale University. [e] Starting strains, obtained from the *E. coli* Genetic Stock Center, Yale University. [f] A gift from Jim Fuchs, Department of Biochemistry, University of Minnesota.

taken. This period was necessary to obtain stable readings and minimize light scattering effects arising from mixing of the bacteria. The substrate was *p*-nitrophenyl phosphate, and the product, *p*-nitrophenol, was monitored by its yellow color at 410 nm. Unless indicated otherwise, the assay buffer was 0.1 M MOPS, pH 7.2, containing 86 mM NaCl plus 1 mM $MgCl_2$. The measured extinction coefficient for *p*-nitrophenol in MOPS buffer at pH 7.2 was 7800 M^{-1} cm^{-1}. In a few experiments, the assay buffer consisted of 0.1 M Tris, pH 8.1, and contained 86 mM NaCl plus 1 mM $MgCl_2$. In this case, the measured extinction coefficient of *p*-nitrophenol was 1.1 $\times$ 10^4 M^{-1} cm^{-1}. Best fit linear analysis of kinetic data was obtained with Macintosh Cricket Graph regression fit.

Enzyme activity that had been released from the periplasm as a result of resuspension of intact cells into assay buffer was subtracted as background. A sample of the resuspended cells used for kinetic studies was centrifuged at 13000*g* for 5 min, and the supernatant was assayed with 3.8 mM substrate. Any activity was subtracted from the experimental readings, as background, prior to plotting the kinetic results. The highest level of released enzyme was 5% of total activity, and, in most cases, there was no detectable enzyme released. In addition, there was no correlation between enzyme released and the concentration of enzyme per cell.

Strain Construction. Strain MZ9387 pIV26 has been described previously (Schendel et al., 1989). Strains M464E, M703CE, and M1157FC were constructed for this study. Starting strains and their genotypes are listed in Table I. Uninduced expression of alkaline phosphatase was eliminated by making all strains *pho A⁻*. The *pho A* deletion was accomplished by P1 (phage) transduction. The P1 lysate used for introducing the *pho A* deletion was obtained from Mark Williams, University of Minnesota, contained the *phoA* deletion, and had the following genotype, grown on BW/3990: *tetʳ, DE(lac)x74, phoM(wt), Δ(zaj, phoA, proC)112::Tn5–132*. All P1 transductions were conducted as follows. Overnight cultures (10 mL of LB) were centrifuged 10 min at 3000*g* and then resuspended in an equal volume of fresh LB broth containing 10 mM $MgCl_2$ and 5 mM $CaCl_2$. The resuspended cells were placed in a shaker (300 rpm) at 37 °C for approximately 20 min. P1 lysates (1–5 μL) were added to sterile tubes containing 100 μL of LB with 10 mM $MgCl_2$ and 5 mM $CaCl_2$. Cells (100 μL) were added to the P1 mixture, and phage absorption to the cells was achieved by incubation for approximately 20 min at 37 °C without shaking. Sodium citrate (100 μL of 1 M) was added to the tubes, and the mixture was then plated out into selection plates containing 15 μg/mL tetracycline. Plates were incubated overnight and examined the next day for transductants (Miller, 1972). An alternative method for detection of P1 transductants involved serial dilutions of the transduced cells, followed by growth on phosphate free MOPS agar plates (with additions). Selection was accomplished by spraying colonies with a 0.25% 5-bromo-4-chloro-3-indoyl phosphate solution.

Since the plasmid, pIV26, can be present in high copy number, it was necessary to have sufficient lac repressor protein in the cells to avoid constitutive synthesis of alkaline phosphatase. This was accomplished through conjugation using strain JF1150, which carriers an F' plasmid containing [*lacIq lacZ::Tn5 Kmʳ*]. Strains to be mated were grown overnight in LB broth at 30 °C with shaking at approximately 100 rpm. Fresh LB broth was inoculated from the overnight cultures and placed in a shaker with the same conditions as overnight cultures. When growth was apparent, 0.5 mL of the two cultures was placed in a sterile tube, and conjugation was accomplished by allowing the mixed cultures to stand for 1 h at 30 °C without shaking. Approximately 200 μL of the cells was spread out on selection plates. Successful conjugation was detected by using plates containing 50 μg/mL kanamycin to detect the presence of *lacIq* and 15 μg/mL tetracycline for selection of cells containing the *pho A* deletion.

Cells were then transformed with the pIV26 plasmid, which contains the *pho A* gene linked to the lac promoter and an ampicillin resistance marker. For plasmid transformations, overnight cultures were centrifuged for 5 min at 12000*g*. Cells were resuspended in 60 mM $CaCl_2$ to one-tenth the original volume and put on ice for 20 min. The cells were then centrifuged for 5 min at 12000*g* and resuspended in 60 mM $CaCl_2$ to 0.02 times the original volume. The cells were allowed to stand in ice for either 1 h or overnight. Competent cells (200 μL) were transferred to a sterile tube to which 1.0 μL of plasmid was added, and the mixture was allowed to stand on ice for 0.5 h. The tube was placed in a water bath (42 °C) for 90 s and then immediately put on ice. Fresh media (0.5 mL of SOC) was added to the cells, and they were placed in an incubator at 37 °C for 1 h. Cells (50 μL) were plated out on ampicillin selection plates, incubated overnight at 37 °C, and examined for transformants the next day (Cohen et al., 1972). Porins present in the three mutant strains were as reported in their respective genotypes (Table I).

Description of Enzyme Kinetics. A simple enzyme-catalyzed reaction can be described by Michaelis–Menten

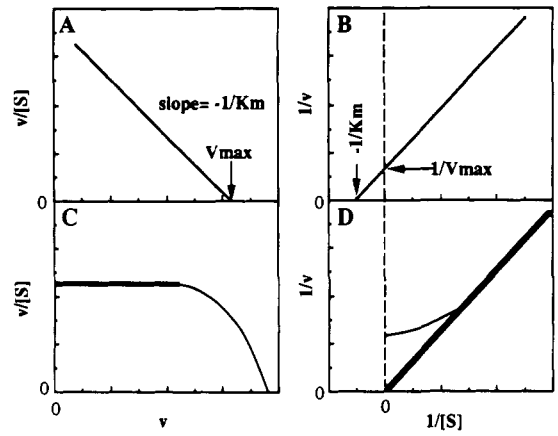

FIGURE 1: Anticipated plots of enzyme kinetic data. Panels A and B are Eadie-Hofstee and Lineweaver–Burk plots, respectively, for Michaelis–Menten type kinetics. Panels C and D are representations of Eadie–Hofstee and Lineweaver–Burk plots expected for a population of enzymes that is functioning at the diffusional limit. The horizontal portion of panel C and extrapolation through zero in panel D illustrate kinetic behavior described by eq 3a. The actual behavior of this system may correspond to the curved line drawn in panel D.

kinetics using standard representations for enzyme, substrate, and product:

$$[E] + [S] \underset{k_{-1}}{\overset{k_1}{\rightleftharpoons}} [E^*S] \xrightarrow{k_2} [E] + [P] \qquad (1)$$

where

$$K_m = \frac{k_2 + k_{-1}}{k_1}$$

Standard plots of kinetic results, such as Lineweaver–Burk and Eadie-Hofstee, will appear as shown in Figure 1, panels B and A, respectively, and constants, such as K_m and V_{max}, can be determined from these plots.

In biological systems there exist factors, such as dense enzyme populations and diffusion barriers, which may alter these kinetic expressions. In this investigation it was necessary to derive an alternative equation (eq 2) to describe the kinetic

$$[S] \underset{k_r}{\overset{k_f}{\rightleftharpoons}} [[E] + [S]' \underset{k_{-1}}{\overset{k_1}{\rightleftharpoons}} [E^*S] \xrightarrow{k_2} [E] + [P]]_n \qquad (2)$$

behavior of the compartmentalized enzymes.

In eq 2, k_f and k_r are rate constants that represent diffusion of the substrate from solution [S], past the diffusion barrier provided by the outer membrane, and into the periplasm [S]′. The enzyme, alkaline phosphatase, exists as a population of enzymes (n) in the periplasm. The events within the brackets of eq 2 are represented by Michaelis–Menten kinetics.

From this expression (eq 2), it is apparent that two extremes can exist. The first extreme occurs when velocity is limited by k_f[S]. This will occur when substrate concentrations are low and free (unbound) enzyme concentrations in the periplasm are high. Each substrate molecule that enters the periplasm will bind to an enzyme and be converted to a product. Escape of substrate from the periplasm (k_r[S]′, eq 2) will be negligible. In this case, the periplasm is acting as a perfectly reactive vessel, and the velocity of the reaction will be a function of cell number rather than of total enzyme concentration. As the bulk substrate concentration is increased, the concentration of substrate in the periplasm will increase until it reaches a point where it is in equilibrium with substrate in bulk solution (i.e., k_r[S]′ is rapid compared to k_2[E*S]). In this case product formation is not limited by k_f[S], and normal Michaelis–Menten kinetics, governed entirely by the expression in the brackets of eq 2, will be observed.

A more precise description of a related phenomenon was provided by Berg and Purcell (1977), who showed that association rate constants consist of the product of two terms. The first term consists of collision between particles and is described by Smoluchowski's theory for collision between two spheres, $k_f = 4\pi N_A Da/1000$, where D is the sum of the diffusion constants of the colliding spheres, a is the sum of the radii, and N_A is Avogadro's number (Smoluchowski, 1917). Upon collision, subsequent binding is a probability, $Ns/(Ns + \pi a)$, where N is the number of vacant binding sites on the particle and s is the effective radius of a binding site. Equation 3 presents a modification of the Berg and Purcell model where

$$k_{f(obs)} = \left(\frac{4\pi N_A D}{1000}\right) af(a) \left(\frac{Nsf(s)}{Nsf(s) + \pi af(a)}\right) \qquad (3)$$

f(a) corrects the Smoluchowski term "a" for the portion of particle collisions that result in entry of substrate into the periplasm, and f(s) corrects the binding site radius for the proportion of binding events that result in product formation. f(s) should equal $k_2/(k_2 + k_{-1})$.

It is important to note that N equals the number of free enzymes rather than total enzymes per cell. Two extremes can be seen in this expression. If $Nsf(s) \gg \pi af(a)$, the probability term for binding between substrate and enzyme approaches 1, and reaction velocity will depend on substrate and cell concentration as given by

$$v = \left(\frac{4\pi N_A Da}{1000}\right) f(a)[S][cell] \qquad (3a)$$

This kinetic behavior will occur at low substrate concentrations on the outside of the cell, where enzyme in the periplasm is largely in the free or vacant form. The periplasm may behave as a perfectly reactive vessel, and each molecule of substrate that enters will be converted to product. Velocity will be proportional to substrate concentration, as long as the number of free enzyme sites remains large. These conditions will produce Eadie–Hofstee plots of zero slope (Figure 1C) and Lineweaver-Burk plots that extrapolate to 0 ($V_{max} = \infty$, Figure 1D).

The second extreme, where $\pi af(a) \gg Nsf(s)$, will occur when the substrate concentration is high. Under these conditions, N, the unoccupied enzyme sites, becomes small, and velocity will be described by

$$v = \left(\frac{4N_A Ds}{1000}\right) f(s)[E][S] \qquad (3b)$$

$k_{f(obs)}$ depends on s and becomes synonymous with k_1. The behavior of the enzyme at this extreme will then approach normal Michaelis–Menten kinetics and will give standard plots such as those in Figure 1A,B. Appropriate substitution of terms in eq 3b results in the expression for steady-state kinetics $v = k_2$(E*S). An important consequence of these behaviors is that the two extremes, as well as all intermediate stages, can be reached within the same titration curve so that Eadie–Hofstee and Lineweaver–Burk plots will become curved (Figure 1C,D) rather than linear. This was shown to be the case for the enzyme system examined in this study.

RESULTS

Cell Growth, Induction, and Free Enzyme Activity. The high levels of alkaline phosphatase expressed in many *E. coli* strains did not cause alteration of bacterial growth. Growth

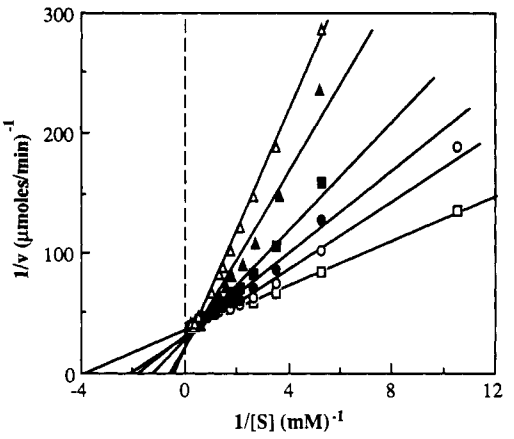

FIGURE 2: Lineweaver–Burk plots of whole cell enzyme kinetic data. An overnight culture was used to inoculated 5-mL cultures as described under Material and Methods. These cultures were induced with IPTG for different amounts of time ranging from 5 min to 3 h. The cells were harvested and resuspended, and a sample of each was lysed and assayed (3.8 mM substrate) to determine the maximum velocity of the enzyme per 10^8 cells. The enzyme activity per 10^8 cells and apparent K_m obtained from the lines drawn for the various cells were as follows: □, 0.008 μmol/min·10^8 cells, 0.24 mM; ○, 0.016 μmol/min·10^8 cells, 0.39 mM; ●, 0.018 μmol/min·10^8 cells, 0.48 mM; ■, 0.038 μmol/min·10^8 cells, 0.66 mM; ▲, 0.044 μmol/min·10^8 cells, 1.13 mM; △, 0.081 μmol/min·10^8 cells, 1.65 mM. The cell densities were adjusted to give a maximum velocity of approximately 0.026 μmol/min, and cell concentrations in these experiments were 3.3×10^8, 1.6×10^8, 1.4×10^8, 6.8×10^7, 5.9×10^7, and 3.2×10^7, respectively, in a 1 mL assay.

curves for strain MZ9387 pIV26, either induced with IPTG or uninduced, were essentially the same (data not shown), with a doubling time of approximately 40 min at 37 °C in tryptone broth. Maximum enzyme induction was obtained from cells that were first grown overnight at 30 °C and used to inoculate fresh media for growth and induction at 37 °C.

The growth media and conditions were selected to avoid release of alkaline phosphatase from the periplasm. Assays of the growth media after cell harvest showed no detectable alkaline phosphatase activity, suggesting little release of the enzyme during growth. Furthermore, even after being stored overnight, harvested, and resuspended, cells did not release significant amounts of enzyme into the buffer. Thus, enzyme release from intact cells was not a significant factor in the studies presented below.

The K_m of highly purified alkaline phosphatase, determined in MOPS buffer, was approximately 15.4 ± 1.3 μM (standard error value $R = 0.96$, data not shown) and was approximately the same when assays were conducted in the presence of uninduced *E. coli* cells. However, the K_m for enzyme that was released from the periplasm by detergent and toluene was 69.0 ± 5.7 μM (standard error value $R = 0.93$, data not shown). Cell debris plus detergent and toluene appeared to account for the difference from pure enzyme. The apparent K_m for pure enzyme, assayed in the presence of the same amount of lysed, uninduced cells, was 69.9 ± 3.7 μM (standard error value $R = 0.98$, data not shown). V_{max} was unaltered by the cells and detergent. The important conclusions for purposes of this study was that the apparent K_m for the free or released enzyme was 15–70 μM. Most values reported below are far above this range.

Induction of Alkaline Phosphatase and in Vivo Kinetic Properties. Double-reciprocal plots for alkaline phosphatase activity in intact cells that had been induced for different lengths of time, and resuspended in MOPS buffer, are shown in Figure 2. Cell concentrations for this series of experiments

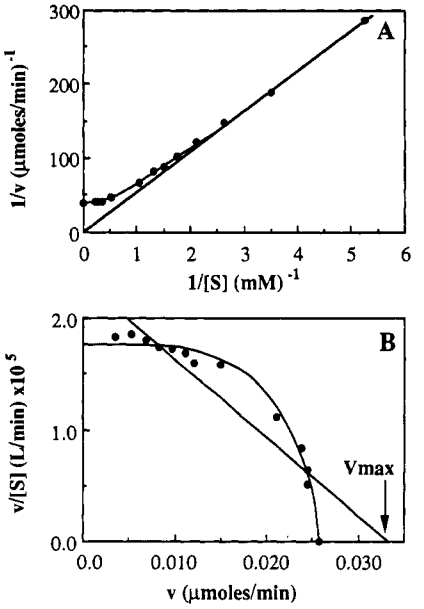

FIGURE 3: Expanded plots of whole cell assays. The data are from the uppermost curve of Figure 2. (Panel A) In the Lineweaver–Burk plot, the straight line drawn correlates with the points at low substrate concentration and extrapolates to zero, as predicted by eq 3a. The points at high substrate concentration begin to deviate toward the V_{max} obtained by enzyme assay of lysed cells (data point at 1/[S] = 0). (Panel B) Eadie–Hofstee plot of the same data. The actual $[S]_{0.5V_{max}}$, obtained from the curved line drawn in panel B, was 0.79 mM. The best fit linear analysis of the data (line shown) corresponds to a V_{max} of 0.033 μmol/min and an apparent K_m of 1.65 mM.

were normalized to give a maximum enzyme velocity of 0.026 μmol/min. In other words, these experiments contained constant total enzyme but variable cell densities. The apparent K_m's for the different cells, obtained as shown, varied from 0.24 to 1.65 mM. The K_m of 1.65 mM was 20–100-fold higher than the K_m of the free or released enzyme. More importantaly, the results showed that a single K_m was inadequate for describing the behavior of this enzyme in whole cells. The K_m showed a dependence on the concentration of enzyme per cell and increased with increasing enzyme density.

Figure 3A shows an expanded Lineweaver–Burk plot of the upper-most plot in Figure 2. While best fit linear analysis gave an apparent K_m of 1.65 mM, closer examination of the data (Figure 3A) showed curvature, indicating more complicated behavior. Linear extrapolation from data points at low substrate passed through zero. At higher substrate, the plot curved toward the true V_{max}, obtained by assay of lysed cells.

Figure 3B is an Eadie–Hofstee plot for the same data. Again the graph might be interpreted in two ways. First, it could be assumed to follow normal Michaelis–Menten kinetics, which should give a straight line plot. The best fit linear analysis gave a V_{max} of 0.038 μmol/min, which was significantly different from V_{max} obtained from lysed cells (0.026 μmol/min). The second way to interpret the data in Figure 3B is with a curved line. In this case, extrapolation gives the correct V_{max}. Thus, the nonlinear curve shape appeared more appropriate. This behavior is predicted by the theory for a diffusion-limited reaction (Figure 1C,D).

Figure 4 shows simple plots of velocity versus substrate concentration, a common way of graphing data from a substrate titration. Superficially, the plots appear to be hyperbolic and characteristic of Michaelis–Menten kinetics. However, the substrate concentrations at $0.5V_{max}$ ($[S]_{0.5V_{max}}$) were different for these three cases which might lead to the

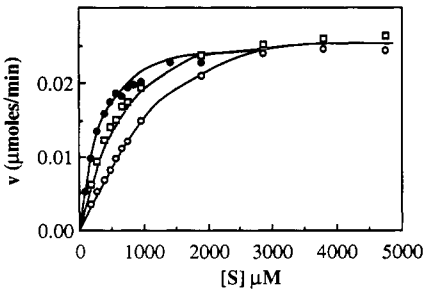

FIGURE 4: Plots of velocity versus substrate concentration. Strain MZ9387 pIV26 was grown and induced for different amounts of time by the standard procedure described under Materials and Methods and in the legend to Figure 2. Cell densities were adjusted to give a maximum enzyme activity (V_{max}) of 0.026 μmol/min. These cultures had different enzyme concentrations per cell that gave V_{max} values, determined after cell lysis, of ●, 0.016 μmol/min·10^8 cells; □, 0.038 μmol/min·10^8 cells; ○, and 0.081 μmol/min·10^8 cells, and the cell concentrations in these experiments were 1.6 × 10^8, 6.8 × 10^7, and 3.2 × 10^7, respectively, in a 1-mL assay.

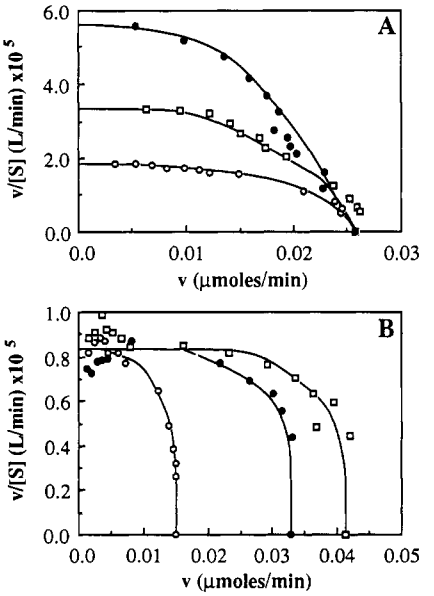

FIGURE 5: Enzyme kinetics at constant enzyme-variable cell concentration (panel A) or constant cell-variable enzyme concentrations (panel B). (Panel A) Eadie–Hofstee plots of kinetic data are shown for cultures with constant total enzyme concentration but variable cell density per assay. The symbols represent the same cultures described in the legend to Figure 4. (Panel B) Kinetics determined using different enzyme concentration but constant cell density per assay. Strain M464E was induced for different periods of time. Assays for the three curves shown contained approximately 6.2 × 10^7 cells. Maximum enzyme velocities for the three cultures in panel B were as follows: ○, 0.019 μmol/min·10^8 cells; ●, 0.055 μmol/mol·10^8 cells; □, 0.069 μmol/min·10^8 cells.

conclusion that three different enzymes were involved. In fact, the three different curves actually arise from the same enzyme but with different concentrations of enzyme per cell. This showed that apparent hyperbolic curve shapes are insufficient to discriminate Michaelis–Menten from diffusion-limited kinetic behavior.

Eadie–Hofstee plots of the data in Figure 4 are shown in Figure 5A. These plots give a better representation of the data and clearly show deviation from linearity. The plots in Figure 5A make it apparent that velocity, at low substrate concentrations, is higher for assays containing a larger number of cells but the same amount of enzyme (left part of Figure 5A). This arises because velocity was described by eq 3a and was a function of cell density rather than enzyme concentration. As expected, cells with a higher enzyme concentration had

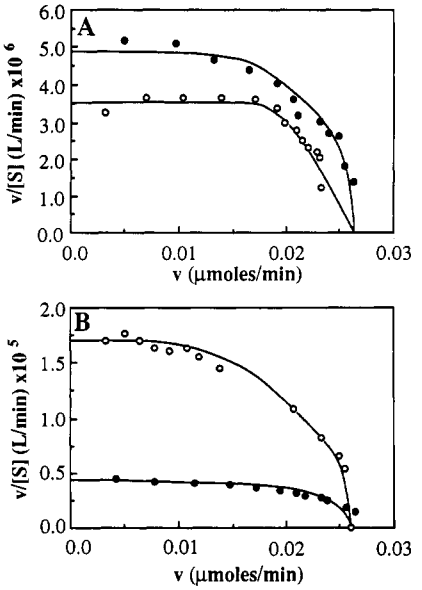

FIGURE 6: Kinetic data for different strains. Media used and induction were as described in Figure 2. (Panel A) Results for M1157FC (●), which expresses Omp F and Omp C, and M464E (○), which expresses only Pho E, are shown. The V_{max} for the M1157FC strain was 0.067 μmol/min·10^8 cells and 0.086 μmol/min·10^8 cells for the M464E strain. Cell concentrations were adjusted to give a V_{max} of 0.026 μmol/min. (Panel B) Plots are of kinetic data obtained with M1157FC (●) and MZ9387 (○). The V_{max} was 0.083 μmol/min·10^8 cells and was the same for both cultures (i.e., enzyme concentration per cell was the same).

kinetics that were governed by diffusion over a larger portion of the graph (i.e., a more extended horizontal region, Figure 5A). This was due to the fact that the number of free enzyme sites per cell remained large enough, over a large range of substrate concentration, to maintain the periplasm as a perfectly reactive vessel that captured every substrate that entered.

Properties of Other E. coli Strains. Experiments in Figures 2–5A used strain MZ9387 pIV26 (Table I). Since this strain lacked the *pho R* gene, it constitutively synthesized the pho E porin, which provided much greater permeability to phosphate-containing compounds. It was of interest to see whether strains with other outer membrane porin combinations would display the same type of diffusion-limited kinetics. Other mutant strains were constructed, and their genotypes are listed in Table I. The strain designation number is followed by letters that signify the possible porins present.

A prediction of the diffusional limited theory is that, at low substrate concentrations, velocity will be a function of cell density rather than enzyme concentration. To confirm this, cell densities for strain M464E were matched for cultures containing different amounts of enzyme (Figure 5B). As predicted, velocities at low substrate concentrations were essentially the same, and velocity was a function of cell number (eq 3a). At high substrate concentrations, the curves shifted toward their true V_{max}, as determined by cell lysis, which was different for the three different cultures.

Figure 6A shows typical curves obtained using two mutant strains, M464E and M1157FC. Since each of these strains should be less permeable for phosphate-containing compounds, the results should demonstrate an even more pronounced diffusion-limited kinetic behavior. This was observed. That is, velocity was proportional to substrate concentration over a larger range, resulting in an extended horizontal region of the graph (Figure 6A). Thus, the behavior described for the

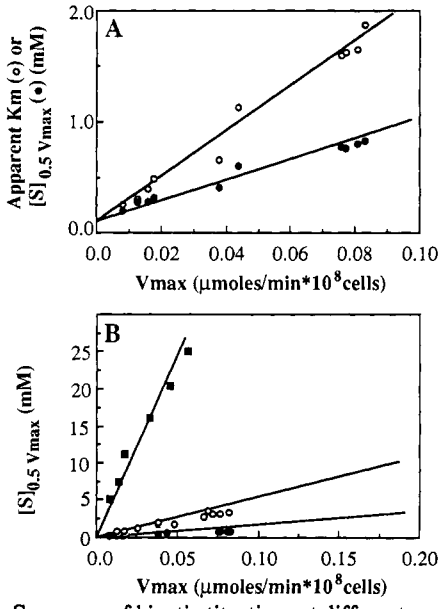

FIGURE 7: Summary of kinetic titrations at different enzyme levels ($V_{max}/10^8$ cells). (Panel A) The K_m values (O) obtained from a series of experiments such as those in Figures 2 and 3 are shown. The K_m was obtained by the best fit linear analysis of kinetic data. Alternatively, $[S]_{0.5V_{max}}$ was determined from the best fit curved line as described in the legend to Figure 3 (●). (Panel B) $[S]_{0.5V_{max}}$ as a function of $V_{max}/10^8$ cells is shown for strains M703CE (■), M1157FC (O), and MZ9387 (●). These strains were selected to illustrate a large variation in outer membrane permeability.

MZ9387 pIV26 strain was even more easily shown for other strains.

A more drastic difference in outer membrane permeability is illustrated in Figure 6B. Eadie–Hofstee plots for strains M1157FC and MZ9387, containing the same enzyme concentration per cell, are shown. Differences in outer membrane permeability can be easily observed by comparison of the left portion of the graphs. Cells with less permeability showed more extended horizontal portions of the graph, indicating that velocity remained proportional to substrate concentration over a larger substrate concentration range. Since enzyme concentration per cell was the same for both sets of data, a more extended horizontal region had to arise from a more restrictive outer membrane [a smaller f(a), eq 3a]. Since these cells contained the same amount of enzyme per cell, the position of the horizontal graph can give an immediate indication of relative outer membrane permeability. These two strains displayed a 4-fold difference in outer membrane permeability.

Since it was clear that K_m is not an accurate constant for these enzyme systems, an alternative value was used. Normally, K_m is the substrate concentration at $0.5V_{max}$. The same experimental value can still be used with the proviso that $[S]_{0.5V_{max}}$ is obtained as the best value from the curved plot rather than analysis of the data by linear equations. Furthermore, unlike K_m, $[S]_{0.5V_{max}}$ cannot be used to predict reaction characteristics at any other substrate concentration. Kinetics were determined for strain MZ9387 pIV26, but at three different cell concentrations. As expected, the maximum velocity increased in proportion to cell concentration, and [v]/[S] increased as well. The $[S]_{0.5V_{max}}$ was essentially the same for all three cell concentrations (approximately 0.3 mM, data not shown). The result showed that $[S]_{0.5V_{max}}$ was independent of cell density and could be used as a reference term for comparing enzyme kinetics in various whole cell assays.

$[S]_{0.5V_{max}}$ values are plotted in Figure 7A as a function of $V_{max}/10^8$ cells, which is a measure of enzyme concentration per cell (strain MZ9387). This graph demonstrates that this value increased linearly with enzyme density per cell. Direct proportionality was expected if $[S]_{0.5V_{max}}$ were limited by diffusion over the entire range of enzyme concentrations. If the same data were analyzed by the Michaelis–Menten equation using the best straight line through the data points, K_m values were also variable (Figure 7A). While we have shown that analysis in this latter manner was not appropriate, this result is presented to demonstrate that, regardless of how the data were analyzed, this system showed a strong dependence between substrate titration curves and the number of enzymes per cell.

Comparisons of strains with different outer membrane permeability can be shown by graphing the experimentally determined $[S]_{0.5V_{max}}$ versus $V_{max}/10^8$ cells (Figure 7B). Results are shown for strains MZ9387 pIV26, M1157FC, and M703CE. A preliminary assessment of outer membrane permeability can be appreciated. All mutants showed a linear increase in $[S]_{0.5V_{max}}$ with enzyme concentration per cell, a result expected for diffusion-limited kinetics. An additional feature was the great difference in the slopes of these curves, indicating a significant difference in outer membrane permeability of these strains. The results were consistent with the expected properties of the porins that are reported to be expected in these strains. MZ9387 showed the greatest permeability and contained a high level of Pho E, the most permeable porin for phosphate-containing compounds. M1157FC showed less permeability because it contained no Pho E porin. Finally, M703CE showed extremely low permeability because it did not contain the Omp F porin and did not express Pho E under these growth conditions. Overall, the differences in permeability (slope of the curves) was greater than 80-fold. This plot provided another method to evaluate outer membrane permeability for various strains and growth conditions.

Kinetics for Wild-Type E. coli. Diffusionally limited kinetics have been demonstrated under conditions of high enzyme concentrations per cell (above), and it was desirable to verify the physiological relevance of this phenomenon. Wild-type *E. coli* strain K12 was grown under conditions of phosphate starvation, and kinetics for normal levels of alkaline phosphatase were determined (Figure 8). Both Eadie–Hofstee and Lineweaver–Burk plots illustrated behavior predicted for the diffusional limit. Cells behaved as perfectly reactive vessels at low substrate concentrations and shifted to Michaelis–Menten type kinetics at high substrate concentrations. These results suggested that the diffusional limit for compartmentalized enzymes was physiologically relevant and may be important for uptake of nutrients by cells where substrate concentrations are likely to be low.

The $[S]_{0.5V_{max}}$ for the wild-type *E. coli* was 0.24 mM, somewhat below the value estimated for the M1157FC (0.5 mM) at the same V_{max} [0.007 μmol/min·10^8 cells, from the straight line (Figure 7B)]. The M1157FC should represent wild-type porins for cells with adequate phosphate. Thus, the result suggested that this wild-type *E. coli* had expressed at least some Pho E porin, thereby increasing the permeability of its outer membrane to a phosphate compound.

Influence of Outer Membrane Damage. The MOPS buffer system used in this study was adopted when it was found that several mutant strains of *E. coli*, which lacked one or more of the outer membrane porins, were very sensitive to Tris buffer and discharged up to 75% of the alkaline phosphatase upon resuspension. Thus, the Tris buffer system appeared to

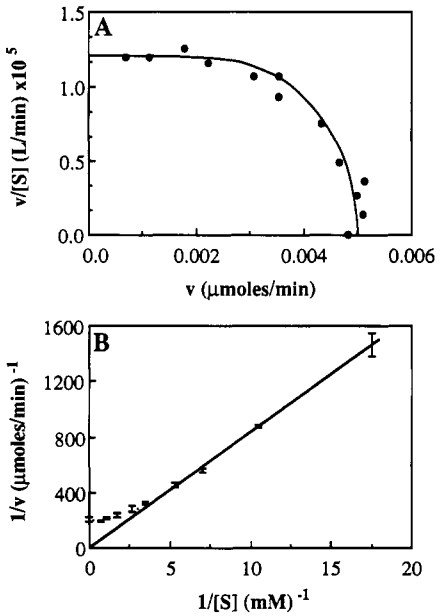

FIGURE 8: In vivo kinetics of alkaline phosphatase in wild type *E. coli*, strain K12. (Panel A) An Eadie–Hofstee plot of whole cell alkaline phosphatase assays for *E. coli* strain K12 is shown. (Panel B) Lineweaver–Burk plot of the same data showing standard deviation for three replicate determinations. Assays contained 0.747×10^8 cells, and V_{max} was 7.0 nmol/min·10^8 cells.

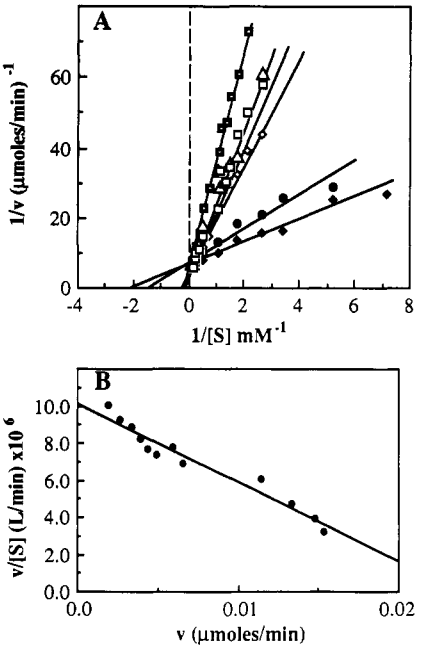

FIGURE 9: Kinetic properties of enzyme in the periplasm with assays conducted in Tris buffer. Cell growth, enzyme induction, and V_{max} determinations were as described under Materials and Methods and in the legend to Figure 2. The cell densities were adjusted to give a maximum velocity of 0.018 μmol/min. Cells were resuspended in Tris buffer. Apparent K_m's were determined from the best linear fit of the data. (Panel A) The enzyme activity per 10^8 cells and apparent K_m's were as follows: ◆, 0.029 μmol/min·10^8 cells, 0.49 mM; ●, 0.104 μmol/min·10^8 cells, 0.78 mM; ◇, 0.301 μmol/min·10^8 cells, 3.9 mM; △, 0.251 μmol/min·10^8 cells, 5.1 mM; □, 0.32 μmol/min·10^8 cells, 7.7 mM; ■, 0.49 μmol/min·10^8 cells, 12.3 mM. The maximum velocity determined from lysed cells used in the assay was 0.018 μmol/min. (Panel B) Eadie–Hofstee graph of data obtained from strain MZ9387 pIV26 resuspended in Tris buffer. The straight line shown corresponds to a V_{max} of 0.024 μmol/min.

damage the outer membrane in these mutant strains. In what might be a related observation, Tris buffer has been reported to sensitize bacteria to lysozyme (Irwin et al., 1981). This could also result from damaging the outer membrane. In contrast, the *E coli* mutants were found to be stable in MOPS buffer and lost less than 5% of the enzyme activity after being washed and resuspended (data not shown).

Strain MZ9387 had appeared stable in the Tris buffer and released less than 5% of the periplasmic enzyme into this buffer upon resuspension. Thus, many early experiments using MZ9387 were carried out in Tris, and a subtle influence of Tris on this strain had been undetected. Figure 9A shows some of these earlier results. The apparent K_m's for the different cells, obtained from the straight lines shown, varied widely from 0.49 to 12.3 mM. The K_m of 12.3 mM was 200–1000-fold higher than the K_m for the free or released enzyme. Qualitatively, the results in Figure 9A were similar to those obtained in MOPS buffer (Figure 2), where the apparent K_m's also varied with enzyme concentration per cell.

Figure 9B shows an Eadie–Hofstee plot for an experiment conducted in Tris buffer. The data conformed to a straight line. The best linear analysis gave an apparent K_m of 2.37 mM and a V_{max} of 0.024 μmol/min. However, the maximum enzyme activity, determined after cell lysis, was 0.018 μmol/min. Clearly, even though the graph appeared linear, more complicated factors were present. It appeared that Tris might have altered the outer membrane of these cells in a minor fashion that gave a mixture of outer membrane permeabilities and heterogeneous diffusion barriers for different enzyme populations. This might contribute to an overall plot that appears linear (Figure 9B). This result was important in that it showed that plots that appear to be linear are inadequate guarantees that the diffusional limit did not apply. Despite this problem, more thorough analysis showed that, even in Tris, the cells still displayed the most important feature of a diffusion-limited reaction, which was variation of apparent K_m as a function of enzyme concentration in the periplasm.

In our preliminary report (Martinez et al., 1992), experiments utilized Tris buffer, and we reported somewhat complex behavior. More complete analysis presented here has simplified the system and identified the source of complexity: subtle damage to the outer membrane by the Tris buffer system.

DISCUSSION

Enzymes are often described by kinetic expressions that are derived for single, free enzymes in dilute solution. These situations do not take into account a number of factors of the in vivo environment. In this study, we were able to demonstrate that the outer membrane of *E. coli* functioned as a diffusion barrier which, combined with dense enzymes in the periplasm, altered kinetic behavior so that conditions for Michaelis–Menten type kinetics were not met. For example, the steady-state conditions of Michaelis–Menten require high substrate to enzyme ratios, which will not apply in a diffusion-limited reaction. If diffusion is the rate-limiting factor in the reaction between substrate and a population of enzymes, $[S]_{0.5V_{max}}$ is not a K_m but is a term dependent on the nature of diffusion as well as the number of enzymes in the population. We have also avoided the use of the term "apparent K_m" to describe $[S]_{0.5V_{max}}$ because this usage suggests a close relationship to the usual concept of K_m, a ratio of rate constants. In the intact bacterial system described here, $[S]_{0.5V_{max}}$ would even be insensitive to the presence of several different forms of an enzyme in the periplasm.

Previous studies showed collisionally limited kinetics for a phage receptor (Schwartz, 1976) and for a cell surface receptor for an antigen (Goldstein, 1989). Collisionally limited kinetics

have also been shown for an in vitro protein–membrane binding process (Abbott & Nelsestuen, 1987, 1988) and for an in vitro enzyme system (Gemmell et al., 1990). However, to our knowledge, this type of behavior for an enzyme population in an actual biological situation has not been shown previously.

While it is possible to derive more precise mathematical descriptions of this behavior, such attempts are not presented here. The major purpose of this study was to demonstrate this type of kinetic behavior and to illustrate how it impacts on the shape and outcome of standard kinetic plots. Kinetic expressions have been derived for immobilized enzymes where diffusion to the vicinity of the attached enzymes was shown to greatly alter enzyme behavior (Laidler & Bunting, 1980, Sundaram et al., 1970). While these systems gave curved Lineweaver–Burk and Eadie–Hofstee plots, they did not show the feature of an absolute limit (horizontal Eadie–Hofstee plots) that was observed in our system. Thus, the intact bacterial presented a more dramatic example of a diffusionally limited enzyme-catalyzed reaction.

The feature of an upper limit and horizontal Eadie–Hofstee plot is viewed as the most important and easily quantitated aspect of this kinetic system. This limit can be dealt with in a straightforward manner, allowing comparison between different bacterial strains. The curved regions of the kinetic plot are less important for several reasons: (1) Curvature occurs at high substrate concentrations which are unlikely to be physiologically important; (2) modeling of the curved region requires extensive knowledge of many parameters. For example, diffusion of substrate out of the periplasm becomes a factor as does the k_{cat}, k_1, and k_2 in the periplasm, which may all be different from the values for free enzyme and substrate. For alkaline phosphatase, the product, phosphate, is also an inhibitor, and its rate of diffusion out of the periplasm, plus its rate of import into the cell, will impact on its concentration in the periplasm and its inhibition properties. Thus, while the curved portions of the graphs are characteristic of this type of kinetics, these portions of the graph are dependent on many variables and require much more complex analysis. The limit function, which is highlighted here, is a property of the entire bacterium and its membrane composition. The value obtained from the limit function, $f(a)$, can be viewed as a simple value that characterizes diffusion through the outer membrane.

The mathematical derivation by Berg and Purcell may provide the simplest description of kinetics for ligand binding to receptors on the outer surface of a particle. While enzymes in the periplasm differ from the Berg and Purcell model in that a chemical reaction is involved and that the enzymes are not freely accessible to bulk solution, the Berg and Purcell equation can be modified, as described in eq 3, to correct for these differences. Basically, $f(s)$ serves to correct a simple binding process for subsequent catalysis, and $f(a)$ corrects for the diffusion barrier. While $f(s)$ is a complicated function, the most important quantitative parameter, $f(a)$, is obtained where $Nsf(s) \gg \pi af(a)$ and $f(s)$ cancels from the rate equation. Thus, with modification, the Berg and Purcell equation can be applied to any situation that involves a population of enzymes or receptors which capture a significant proportion of the substrate that diffuses to their region.

The actual value of $f(a)$ can be estimated from the observed diffusion-limited reaction. The rate constant for collision between substrate ($M_w = 217$, $D_{20^w} =$ ca. 5×10^{-6} cm^2/s) and an *E. coli* cell of 1-μm diameter would be about 2.8×10^{12} M^{-1} s^{-1} at 37 °C. This would be the maximum possible rate constant for conversion of substrate to product by an entire bacterium with enzyme freely available on the surface. For the strain MZ9387 pIV26, a diffusion-limited situation existed at a velocity of 0.01 μmol/min (Figure 3B). In combination with the corresponding cell and substrate concentrations, a diffusion-limited second-order rate constant of 5.54×10^9 M^{-1} s^{-1} was estimated. This was 0.20% of the theoretical maximum so that $f(a)$ for this *E. coli* strain, grown as described, was 2.0×10^{-3}. In other words, 0.20% of the collisions between substrate and cells resulted in substrate entry into the periplasm. As expected, $f(a)$ was highly dependent on the porins expressed so that $f(a)$ for strain M1157FC (Figure 6A) was 4.9×10^{-4}. Preliminary results with other strains has shown nearly a 100-fold variation in $f(a)$. The total range of $[S]_{0.5V_{max}}$ was 0.015 mM for free enzyme to 32 mM for the highest enzyme concentration in bacteria with the most restrictive porins (data not shown). In fact, the kinetic system developed in this study offered an excellent method for study of the permeability of the outer membrane of *E. coli* under a wide range of growth conditions and porin expression. Studies to document these parameters are in progress.

Conditions needed to reach the diffusion limit will vary for each substrate. Larger substrates, with smaller $f(a)$, will reach the diffusion limit more readily (fewer enzymes in the periplasm) than smaller substrates. In addition, substrates for which the enzyme has a high k_{cat} value will reach the diffusion limit more readily than poor substrates for which the enzyme has a low k_{cat} value. While considerable variation might be expected, it is interesting to speculate that the evolutionary end point for the number of enzymes expressed in the periplasm (or in any other population of enzymes) would be the level needed to reach the perfectly reactive state, the diffusion-limited state, where every substrate that encounters the enzyme population is captured and converted to product. This same criterion may also be the evolutionary end point for expression of some receptors on the cell surface (Abbott & Nelsestuen, 1988). Wild-type *E. coli*, with normal expression levels of alkaline phosphatase showed diffusion-limited kinetics when [S] was low.

Observation of diffusionally limited, compartmentalized enzyme kinetics at the lower enzyme levels in this study suggested other important properties of the periplasm. Given an estimated k_{cat} for free enzyme of 33/s, a cell population with a V_{max} of 0.007 μmol/min·10^8 cells (Figure 8) would contain 2×10^4 enzyme molecules per cell, less than the usual number of porins [about 10^5/cell (Lugtenberg et al., 1976)]. In order for this cell to display diffusion-limited, compartmentalized enzyme kinetics, the compartmentalized enzymes must utilize a common pool of substrate. Assuming random distribution of the larger number of porins on the surface and random localization of the smaller number of enzymes in the periplasm, this situation could only arise if lateral diffusion of substrate in the periplasm was rapid relative to entry, or exit, of substrate to, or from, the periplasm. If lateral diffusion were limiting, each enzyme would be localized to the region of a single porin, and while restricted diffusion of substrate through the porin might cause an increased K_m, it would produce normal Michaelis–Menten kinetics and a single K_m. Thus, the results suggested that the nature of the periplasm allowed lateral diffusion of this substrate that was rapid relative to catalysis, entry to, or exit from, the periplasm.

Several problems can arise if kinetics of the type described here are observed but interpreted from the standpoint of Michaelis–Menten kinetics. Variable K_m's for different conditions might suggest the presence of multiple enzymes. The nearly horizontal region of the Eadie–Hofstee plot, with

linear extrapolation to obtain V_{max}, would suggest an extremely abundant enzyme with high K_m. However, upon release of the enzyme from the cells, this abundant enzyme would seem to disappear. If a preparation contains a mixture of free enzymes and compartmentalized enzymes, the result would suggest two enzymes, one with a high K_m and another with a low K_m. However, the high K_m form of the enzyme would disappear upon more complete disruption of the cells. These properties simply reiterate the fact that enzyme properties, in situ, may be quite different from those observed for free enzymes.

An additional precaution was suggested by the results obtained with Tris buffer. Tris buffer had an easily detected adverse affect on cell lines with altered outer membranes. However, even though Tris did not cause extensive release of the enzyme from the MZ9387 pIV26 strain, it caused enough damage to partially mask some of the properties of diffusion-limited kinetics. On initial inspection, the Eadie–Hofstee and Lineweaver–Burk plots often appeared linear and adequate to obtain apparent K_m and V_{max}. However, closer examination of the data suggested that something was wrong. The V_{max} was higher than it should have been, and the K_m varied with the number of enzymes per cell. Thus, observation of linear plots was an insufficient criterion to rule out a diffusion-limited, compartmentalized enzyme system. Failure to test whole cell assays under different conditions may mask diffusionally limited systems, and conclusions drawn may be in error.

Whole cells have been used in bioprocessing for conversion of substrate to product such as conversion of DL-serine to L-tryptophan (Ishiwata et al., 1990). Diffusion-limited kinetics of compartmentalized enzymes may also impact on the potential use of periplasmic enzymes of Gram-negative bacteria for bioprocessing. That is, at the diffusional limit, reaction velocity becomes a function of cell number and membrane permeability rather than enzyme concentration. In this system, overexpression of enzymes in the periplasm may give limited benefit unless the substrate concentration is very high.

That whole cell systems may frequently display this behavior is further illustrated by oligobacteria. These oceanic bacteria grow at extremely low substrate concentrations and appear to express high levels of substrate receptors on their surface. This provides the maximum transport of nutrients to a limited enzyme population inside the cell (Button, 1991). Nutrient uptake at low substrate concentration may even become a function of diffusion rather than a property of the receptor binding site. Densely populated cell surface receptors of other types may serve similar function(s). Many cases exist where enzymes are much more abundant than their substrates, and further studies may show that this may serve to capture substrates before they diffuse away to other parts of the cell. The high concentration of a group of glycolytic enzymes in muscle (0.2–1.0 mM) together with their k_{cat} values (50–500/s) provide extremely high saturation substrate turnover (0.02–1.0 M/s) (Srivastava & Bernhard, 1986). The "excess enzyme" may be used to achieve diffusion-limited kinetics in the cell. Another example might be cGMP-binding proteins of the visual receptors which are present at much higher concentration than cGMP (Dawis et al., 1988). In many cases, a large number of vacant sites (receptors or enzymes) may create diffusion-limited systems, thereby localizing metabolic pathways, second messengers, etc., to regions of the cell. In fact, better understanding of in situ kinetics may reveal cell regulation mechanisms that have gone undetected: cells may regulate enzyme/receptor behavior by altering diffusion barriers or population sizes of the enzymes/receptors.

REFERENCES

Abbott, A. J., & Nelsestuen, G. L. (1987) *Biochemistry 26*, 7994.
Abbott, A. J., & Nelsestuen, G. L. (1988) *FASEB J. 2*, 2858.
Adler, J. (1973) *J. Gen. Microbiol. 74*, 77.
Alphen, W. V., & Lugtenberg, B. (1977) *J. Bacteriol. 131*, 623.
Alphen, W. V., Selm, N. V., & Lugtenberg, B. (1978) *Mol. Gen. Genet. 159*, 75.
Argast, M., & Boos, W. (1980) *J. Bacteriol. 143*, 142.
Beacham, I. R. (1979) *Eur. J. Biochem. 10*, 877.
Berg, H. C., & Purcell, E. M. (1977) *Biophys. J. 20*, 193.
Button, D. K. (1991) *Appl. Environ. Microbiol. 57*, 2033.
Cohen, S. N., Chang, A. C. Y., & Hsu, L. (1972) *Proc. Natl. Acad. Sci. U.S.A. 69*, 2110.
Datta, D. B., Arden, B., & Henning, U. (1977) *J. Bacteriol. 131*, 821.
Dawis, S. M., Graeff, R. M., Heyman, R. A., Walseth, T. F., & Goldberg, N. D. (1988) *J. Biol. Chem. 263*, 8771.
Gemmell, C. H., Nemerson, Y., & Turitto, V. (1990) *Microvasc. Res. 40*, 327.
Goldstein, B. (1989) in *Comments Theoretical Biology* (Blum, J. J., et al., Eds.) Gordon and Breach, Great Britain.
Hanahan, D. (1985) in *DNA Cloning: A Practical Approach* (Glover D. M., Ed.) p 109, IRL Press, Washington, D.C.
Irwin, R. T., MacAlister, T. J., & Costerton, J. W. (1981) *J. Bacteriol. 145*, 1397.
Ishiwata, K. I., Fukuhara, N., Shimada, M., Makiguchi, N., & Soda, K. (1990) *Biotechnol. Appl. Biochem. 12*, 141.
Jovanovich, S. B., Martinell, M., Record, M. T., Jr., & Burgess, R. R. (1988) *J. Bacteriol. 170*, 534.
Korteland, J., Graaff, P. D., & Lugtenberg, B. (1984) *Biochim. Biophys. Acta 778*, 311.
Laidler, K. J., & Bunting, P. S. (1980) *Methods Enzymol. 64*, 397.
Lugtenberg, B., Peters, R., Bernheimer, H., & Berendsen, W. (1976) *Mol. Gen. Genet. 147*, 251.
Martinez, M. B., Schendel, F. J., Flickinger, M. C., & Nelsestuen, G. L. (1992) *FASEB J. 6*, A460.
Miller, J. (1972) in *Experiments in Molecular Genetics*, Cold Spring Harbor Laboratory Press, Cold Spring Harbor, New York.
Nakae, T., Ishii, J., & Tokunaga, M. (1979) *J. Biol. Chem. 254*, 1457.
Neidhardt, F. C., Block, P. L., & Smith, D. F. (1974) *J.* Bacteriol. *119*, 736.
Nikaido, H., & Nakae, T. (1979) *Adv. Microb. Physiol. 20*, 163.
Nikaido, H., & Rosenberg, E. Y. (1983) *J. Bacteriol. 153*, 241.
Nikaido, H., & Vaara, M. (1985) *Microbiol. Rev. 49*, 1.
Schendel, F. J., Baude, E. J., & Flickinger, M. C. (1989) *Biotechnol. Bioeng. 34*, 1023.
Schwartz, M. (1976) *J. Mol. Biol. 103*, 521.
Smoluchowski, M. (1917) *Phys. Chem. Abstr. A 92*, 129.
Srivastava, D. K., & Bernhard, S. A. (1986) *Curr. Top. Cell. Regul. 28*, 1.
Stock, J. B., Rauch, B., & Roseman, S. (1977) *J. Biol. Chem. 252*, 7850.
Sundaram, P. V., Tweedale, A., & Laidler, K. J. (1970) *Can. J. Chem. 48*, 1498.
Tartof, K. D., & Hobbs, S. A. (1987) *Focus 9*, 12.
Tommassen, J., & Lugtenberg, B. (1990) *J. Bacteriol. 143*, 151.
Vaara, M., & Vaara, T. (1983) *Antimicrob. Agents Chemother. 24*, 107.
Zimmerman, W., & Rosselet, A. (1977) *Antimicrob. Agents Chemother. 12*, 368.